

Measurements of Born Cross Sections of $e^+e^- \rightarrow D_s^{*+}D_s^- + c.c.$

M. Ablikim¹, M. N. Achasov^{10,b}, P. Adlarson⁶⁷, S. Ahmed¹⁵, M. Albrecht⁴, R. Aliberti²⁸, A. Amoroso^{66A,66C}, M. R. An³², Q. An^{63,49}, X. H. Bai⁵⁷, Y. Bai⁴⁸, O. Bakina²⁹, R. Baldini Ferroli^{23A}, I. Balossino^{24A}, Y. Ban^{38,i}, K. Begzsuren²⁶, N. Berger²⁸, M. Bertani^{23A}, D. Bettoni^{24A}, F. Bianchi^{66A,66C}, J. Bloms⁶⁰, A. Bortone^{66A,66C}, I. Boyko²⁹, R. A. Briere⁵, H. Cai⁶⁸, X. Cai^{1,49}, A. Calcaterra^{23A}, G. F. Cao^{1,54}, N. Cao^{1,54}, S. A. Cetin^{53A}, J. F. Chang^{1,49}, W. L. Chang^{1,54}, G. Chelkov^{29,a}, D. Y. Chen⁶, G. Chen¹, H. S. Chen^{1,54}, M. L. Chen^{1,49}, S. J. Chen³⁵, X. R. Chen²⁵, Y. B. Chen^{1,49}, Z. J. Chen^{20,j}, W. S. Cheng^{66C}, G. Cibinetto^{24A}, F. Cossio^{66C}, X. F. Cui³⁶, H. L. Dai^{1,49}, X. C. Dai^{1,54}, A. Dbeyssi¹⁵, R. E. de Boer⁴, D. Dedovich²⁹, Z. Y. Deng¹, A. Denig²⁸, I. Denysenko²⁹, M. Destefanis^{66A,66C}, F. De Mori^{66A,66C}, Y. Ding³³, C. Dong³⁶, J. Dong^{1,49}, L. Y. Dong^{1,54}, M. Y. Dong^{1,49,54}, X. Dong⁶⁸, S. X. Du⁷¹, Y. L. Fan⁶⁸, J. Fang^{1,49}, S. S. Fang^{1,54}, Y. Fang¹, R. Farinelli^{24A}, L. Fava^{66B,66C}, F. Feldbauer⁴, G. Felici^{23A}, C. Q. Feng^{63,49}, J. H. Feng⁵⁰, M. Fritsch⁴, C. D. Fu¹, Y. Gao⁶⁴, Y. Gao^{63,49}, Y. Gao^{38,i}, Y. G. Gao⁶, I. Garzia^{24A,24B}, P. T. Ge⁶⁸, C. Geng⁵⁰, E. M. Gersabeck⁵⁸, A. Gilman⁶¹, K. Goetzen¹¹, L. Gong³³, W. X. Gong^{1,49}, W. Gradl²⁸, M. Greco^{66A,66C}, L. M. Gu³⁵, M. H. Gu^{1,49}, S. Gu², Y. T. Gu¹³, C. Y. Guan^{1,54}, A. Q. Guo²², L. B. Guo³⁴, R. P. Guo⁴⁰, Y. P. Guo^{9,g}, A. Guskov^{29,a}, T. T. Han⁴¹, W. Y. Han³², X. Q. Hao¹⁶, F. A. Harris⁵⁶, K. L. He^{1,54}, F. H. Heinsius⁴, C. H. Heinz²⁸, T. Held⁴, Y. K. Heng^{1,49,54}, C. Herold⁵¹, M. Himmelreich^{11,e}, T. Holtmann⁴, G. Y. Hou^{1,54}, Y. R. Hou⁵⁴, Z. L. Hou¹, H. M. Hu^{1,54}, J. F. Hu^{47,k}, T. Hu^{1,49,54}, Y. Hu¹, G. S. Huang^{63,49}, L. Q. Huang⁶⁴, X. T. Huang⁴¹, Y. P. Huang¹, Z. Huang^{38,i}, T. Hussain⁶⁵, N. Hüsken^{22,28}, W. Ikegami Andersson⁶⁷, W. Imoehl²², M. Irshad^{63,49}, S. Jaeger⁴, S. Janchiv²⁶, Q. Ji¹, Q. P. Ji¹⁶, X. B. Ji^{1,54}, X. L. Ji^{1,49}, Y. Y. Ji⁴¹, H. B. Jiang⁴¹, X. S. Jiang^{1,49,54}, J. B. Jiao⁴¹, Z. Jiao¹⁸, S. Jin³⁵, Y. Jin⁵⁷, M. Q. Jing^{1,54}, T. Johansson⁶⁷, N. Kalantar-Nayestanaki⁵⁵, X. S. Kang³³, R. Kappert⁵⁵, M. Kavatsyuk⁵⁵, B. C. Ke^{43,1}, I. K. Keshk⁴, A. Khoukaz⁶⁰, P. Kiese²⁸, R. Kiuchi¹, R. Kliemt¹¹, L. Koch³⁰, O. B. Kolcu^{53A,d}, B. Kopf⁴, M. Kuemmel⁴, M. Kuessner⁴, A. Kupsc⁶⁷, M. G. Kurth^{1,54}, W. Kühn³⁰, J. J. Lane⁵⁸, J. S. Lange³⁰, P. Larin¹⁵, A. Lavanaia²¹, L. Lavezzi^{66A,66C}, Z. H. Lei^{63,49}, H. Leithoff²⁸, M. Lellmann²⁸, T. Lenz²⁸, C. Li³⁹, C. H. Li³², Cheng Li^{63,49}, D. M. Li⁷¹, F. Li^{1,49}, G. Li¹, H. Li^{63,49}, H. Li⁴³, H. B. Li^{1,54}, H. J. Li¹⁶, J. L. Li⁴¹, J. Q. Li⁴, J. S. Li⁵⁰, Ke Li¹, L. K. Li¹, Lei Li³, P. R. Li^{31,l,m}, S. Y. Li⁵², W. D. Li^{1,54}, W. G. Li¹, X. H. Li^{63,49}, X. L. Li⁴¹, Xiaoyu Li^{1,54}, Z. Y. Li⁵⁰, H. Liang^{63,49}, H. Liang^{1,54}, H. Liang²⁷, Y. F. Liang⁴⁵, Y. T. Liang²⁵, G. R. Liao¹², L. Z. Liao^{1,54}, J. Libby²¹, C. X. Lin⁵⁰, B. J. Liu¹, C. X. Liu¹, D. Liu^{15,63}, F. H. Liu⁴⁴, Fang Liu¹, Feng Liu⁶, H. B. Liu¹³, H. M. Liu^{1,54}, Huanhuan Liu¹, Huihui Liu¹⁷, J. B. Liu^{63,49}, J. L. Liu⁶⁴, J. Y. Liu^{1,54}, K. Liu¹, K. Y. Liu³³, L. Liu^{63,49}, M. H. Liu^{9,g}, P. L. Liu¹, Q. Liu⁶⁸, Q. Liu⁵⁴, S. B. Liu^{63,49}, Shuai Liu⁴⁶, T. Liu^{1,54}, W. M. Liu^{63,49}, X. Liu^{31,l,m}, Y. Liu^{31,l,m}, Y. B. Liu³⁶, Z. A. Liu^{1,49,54}, Z. Q. Liu⁴¹, X. C. Lou^{1,49,54}, F. X. Lu⁵⁰, H. J. Lu¹⁸, J. D. Lu^{1,54}, J. G. Lu^{1,49}, X. L. Lu¹, Y. Lu¹, Y. P. Lu^{1,49}, C. L. Luo³⁴, M. X. Luo⁷⁰, P. W. Luo⁵⁰, T. Luo^{9,g}, X. L. Luo^{1,49}, X. R. Lyu⁵⁴, F. C. Ma³³, H. L. Ma¹, L. L. Ma⁴¹, M. M. Ma^{1,54}, Q. M. Ma¹, R. Q. Ma^{1,54}, R. T. Ma⁵⁴, X. X. Ma^{1,54}, X. Y. Ma^{1,49}, F. E. Maas¹⁵, M. Maggiora^{66A,66C}, S. Maldaner⁴, S. Malde⁶¹, Q. A. Malik⁶⁵, A. Mangoni^{23B}, Y. J. Mao^{38,i}, Z. P. Mao¹, S. Marcello^{66A,66C}, Z. X. Meng⁵⁷, J. G. Messchendorp⁵⁵, G. Mezzadri^{24A}, T. J. Min³⁵, R. E. Mitchell²², X. H. Mo^{1,49,54}, Y. J. Mo⁶, N. Yu. Muchnoi^{10,b}, H. Muramatsu⁵⁹, S. Nakhoul^{11,e}, Y. Nefedov²⁹, F. Nerling^{11,e}, I. B. Nikolaev^{10,b}, Z. Ning^{1,49}, S. Nisar^{8,h}, S. L. Olsen⁵⁴, Q. Ouyang^{1,49,54}, S. Pacetti^{23B,23C}, X. Pan^{9,g}, Y. Pan⁵⁸, A. Pathak¹, A. Pathak²⁷, P. Patteri^{23A}, M. Pelizaeus⁴, H. P. Peng^{63,49}, K. Peters^{11,e}, J. Pettersson⁶⁷, J. L. Ping³⁴, R. G. Ping^{1,54}, S. Pogodin²⁹, R. Poling⁵⁹, V. Prasad^{63,49}, H. Qi^{63,49}, H. R. Qi⁵², K. H. Qi²⁵, M. Qi³⁵, T. Y. Qi⁹, S. Qian^{1,49}, W. B. Qian⁵⁴, Z. Qian⁵⁰, C. F. Qiao⁵⁴, L. Q. Qin¹², X. P. Qin⁹, X. S. Qin⁴¹, Z. H. Qin^{1,49}, J. F. Qiu¹, S. Q. Qu³⁶, K. H. Rashid⁶⁵, K. Ravindran²¹, C. F. Redmer²⁸, A. Rivetti^{66C}, V. Rodin⁵⁵, M. Rolo^{66C}, G. Rong^{1,54}, Ch. Rosner¹⁵, M. Rump⁶⁰, H. S. Sang⁶³, A. Sarantsev^{29,c}, Y. Schelhaas²⁸, C. Schmier⁴, K. Schoenning⁶⁷, M. Scodeggio^{24A,24B}, D. C. Shan⁴⁶, W. Shan¹⁹, X. Y. Shan^{63,49}, J. F. Shangguan⁴⁶, M. Shao^{63,49}, C. P. Shen⁹, H. F. Shen^{1,54}, P. X. Shen³⁶, X. Y. Shen^{1,54}, H. C. Shi^{63,49}, R. S. Shi^{1,54}, X. Shi^{1,49}, X. D. Shi^{63,49}, J. J. Song⁴¹, W. M. Song^{27,1}, Y. X. Song^{38,i}, S. Sosio^{66A,66C}, S. Spataro^{66A,66C}, K. X. Su⁶⁸, P. P. Su⁴⁶, F. F. Sui⁴¹, G. X. Sun¹, H. K. Sun¹, J. F. Sun¹⁶, L. Sun⁶⁸, S. S. Sun^{1,54}, T. Sun^{1,54}, W. Y. Sun²⁷, W. Y. Sun³⁴, X. Sun^{20,j}, Y. J. Sun^{63,49}, Y. K. Sun^{63,49}, Y. Z. Sun¹, Z. T. Sun¹, Y. H. Tan⁶⁸, Y. X. Tan^{63,49}, C. J. Tang⁴⁵, G. Y. Tang¹, J. Tang⁵⁰, J. X. Teng^{63,49}, V. Thoren⁶⁷, W. H. Tian⁴³, Y. T. Tian²⁵, I. Uman^{53B}, B. Wang¹, C. W. Wang³⁵, D. Y. Wang^{38,i}, H. J. Wang^{31,l,m}, H. P. Wang^{1,54}, K. Wang^{1,49}, L. L. Wang¹, M. Wang⁴¹, M. Z. Wang^{38,i}, Meng Wang^{1,54}, W. Wang⁵⁰, W. H. Wang⁶⁸, W. P. Wang^{63,49}, X. Wang^{38,i}, X. F. Wang^{31,l,m}, X. L. Wang^{9,g}, Y. Wang^{63,49}, Y. Wang⁵⁰, Y. D. Wang³⁷, Y. F. Wang^{1,49,54}, Y. Q. Wang¹, Y. Y. Wang^{31,l,m}, Z. Wang^{1,49}, Z. Y. Wang¹, Ziyi Wang⁵⁴, Zongyuan Wang^{1,54}, D. H. Wei¹², F. Weidner⁶⁰, S. P. Wen¹, D. J. White⁵⁸, U. Wiedner⁴, G. Wilkinson⁶¹, M. Wolke⁶⁷, L. Wollenberg⁴, J. F. Wu^{1,54}, L. H. Wu¹, L. J. Wu^{1,54}, X. Wu^{9,g}, Z. Wu^{1,49},

L. Xia^{63,49}, H. Xiao^{9,g}, S. Y. Xiao¹, Z. J. Xiao³⁴, X. H. Xie^{38,i}, Y. G. Xie^{1,49}, Y. H. Xie⁶, T. Y. Xing^{1,54}, G. F. Xu¹, Q. J. Xu¹⁴, W. Xu^{1,54}, X. P. Xu⁴⁶, Y. C. Xu⁵⁴, F. Yan^{9,g}, L. Yan^{9,g}, W. B. Yan^{63,49}, W. C. Yan⁷¹, Xu Yan⁴⁶, H. J. Yang^{42,f}, H. X. Yang¹, L. Yang⁴³, S. L. Yang⁵⁴, Y. X. Yang¹², Yifan Yang^{1,54}, Zhi Yang²⁵, M. Ye^{1,49}, M. H. Ye⁷, J. H. Yin¹, Z. Y. You⁵⁰, B. X. Yu^{1,49,54}, C. X. Yu³⁶, G. Yu^{1,54}, J. S. Yu^{20,j}, T. Yu⁶⁴, C. Z. Yuan^{1,54}, L. Yuan², X. Q. Yuan^{38,i}, Y. Yuan¹, Z. Y. Yuan⁵⁰, C. X. Yue³², A. A. Zafar⁶⁵, X. Zeng Zeng⁶, Y. Zeng^{20,j}, A. Q. Zhang¹, B. X. Zhang¹, Guangyi Zhang¹⁶, H. Zhang⁶³, H. H. Zhang⁵⁰, H. H. Zhang²⁷, H. Y. Zhang^{1,49}, J. J. Zhang⁴³, J. L. Zhang⁶⁹, J. Q. Zhang³⁴, J. W. Zhang^{1,49,54}, J. Y. Zhang¹, J. Z. Zhang^{1,54}, Jianyu Zhang^{1,54}, Jiawei Zhang^{1,54}, L. M. Zhang⁵², L. Q. Zhang⁵⁰, Lei Zhang³⁵, S. Zhang⁵⁰, S. F. Zhang³⁵, Shulei Zhang^{20,j}, X. D. Zhang³⁷, X. Y. Zhang⁴¹, Y. Zhang⁶¹, Y. T. Zhang⁷¹, Y. H. Zhang^{1,49}, Yan Zhang^{63,49}, Yao Zhang¹, Z. H. Zhang⁶, Z. Y. Zhang⁶⁸, G. Zhao¹, J. Zhao³², J. Y. Zhao^{1,54}, J. Z. Zhao^{1,49}, Lei Zhao^{63,49}, Ling Zhao¹, M. G. Zhao³⁶, Q. Zhao¹, S. J. Zhao⁷¹, Y. B. Zhao^{1,49}, Y. X. Zhao²⁵, Z. G. Zhao^{63,49}, A. Zhemchugov^{29,a}, B. Zheng⁶⁴, J. P. Zheng^{1,49}, Y. Zheng^{38,i}, Y. H. Zheng⁵⁴, B. Zhong³⁴, C. Zhong⁶⁴, L. P. Zhou^{1,54}, Q. Zhou^{1,54}, X. Zhou⁶⁸, X. K. Zhou⁵⁴, X. R. Zhou^{63,49}, X. Y. Zhou³², A. N. Zhu^{1,54}, J. Zhu³⁶, K. Zhu¹, K. J. Zhu^{1,49,54}, S. H. Zhu⁶², T. J. Zhu⁶⁹, W. J. Zhu³⁶, W. J. Zhu^{9,g}, Y. C. Zhu^{63,49}, Z. A. Zhu^{1,54}, B. S. Zou¹, J. H. Zou¹

(BESIII Collaboration)

¹ *Institute of High Energy Physics, Beijing 100049, People's Republic of China*

² *Beihang University, Beijing 100191, People's Republic of China*

³ *Beijing Institute of Petrochemical Technology, Beijing 102617, People's Republic of China*

⁴ *Bochum Ruhr-University, D-44780 Bochum, Germany*

⁵ *Carnegie Mellon University, Pittsburgh, Pennsylvania 15213, USA*

⁶ *Central China Normal University, Wuhan 430079, People's Republic of China*

⁷ *China Center of Advanced Science and Technology, Beijing 100190, People's Republic of China*

⁸ *COMSATS University Islamabad, Lahore Campus, Defence Road, Off Raiwind Road, 54000 Lahore, Pakistan*

⁹ *Fudan University, Shanghai 200443, People's Republic of China*

¹⁰ *G.I. Budker Institute of Nuclear Physics SB RAS (BINP), Novosibirsk 630090, Russia*

¹¹ *GSI Helmholtzcentre for Heavy Ion Research GmbH, D-64291 Darmstadt, Germany*

¹² *Guangxi Normal University, Guilin 541004, People's Republic of China*

¹³ *Guangxi University, Nanning 530004, People's Republic of China*

¹⁴ *Hangzhou Normal University, Hangzhou 310036, People's Republic of China*

¹⁵ *Helmholtz Institute Mainz, Staudinger Weg 18, D-55099 Mainz, Germany*

¹⁶ *Henan Normal University, Xinxiang 453007, People's Republic of China*

¹⁷ *Henan University of Science and Technology, Luoyang 471003, People's Republic of China*

¹⁸ *Huangshan College, Huangshan 245000, People's Republic of China*

¹⁹ *Hunan Normal University, Changsha 410081, People's Republic of China*

²⁰ *Hunan University, Changsha 410082, People's Republic of China*

²¹ *Indian Institute of Technology Madras, Chennai 600036, India*

²² *Indiana University, Bloomington, Indiana 47405, USA*

²³ *INFN Laboratori Nazionali di Frascati, (A)INFN Laboratori Nazionali di Frascati, I-00044, Frascati, Italy; (B)INFN Sezione di Perugia, I-06100, Perugia, Italy; (C)University of Perugia, I-06100, Perugia, Italy*

²⁴ *INFN Sezione di Ferrara, (A)INFN Sezione di Ferrara, I-44122,*

Ferrara, Italy; (B)University of Ferrara, I-44122, Ferrara, Italy

²⁵ *Institute of Modern Physics, Lanzhou 730000, People's Republic of China*

²⁶ *Institute of Physics and Technology, Peace Ave. 54B, Ulaanbaatar 13330, Mongolia*

²⁷ *Jilin University, Changchun 130012, People's Republic of China*

²⁸ *Johannes Gutenberg University of Mainz, Johann-Joachim-Becher-Weg 45, D-55099 Mainz, Germany*

²⁹ *Joint Institute for Nuclear Research, 141980 Dubna, Moscow region, Russia*

³⁰ *Justus-Liebig-Universitaet Giessen, II. Physikalisches Institut, Heinrich-Buff-Ring 16, D-35392 Giessen, Germany*

³¹ *Lanzhou University, Lanzhou 730000, People's Republic of China*

³² *Liaoning Normal University, Dalian 116029, People's Republic of China*

³³ *Liaoning University, Shenyang 110036, People's Republic of China*

³⁴ *Nanjing Normal University, Nanjing 210023, People's Republic of China*

³⁵ *Nanjing University, Nanjing 210093, People's Republic of China*

³⁶ *Nankai University, Tianjin 300071, People's Republic of China*

- ³⁷ North China Electric Power University, Beijing 102206, People's Republic of China
- ³⁸ Peking University, Beijing 100871, People's Republic of China
- ³⁹ Qufu Normal University, Qufu 273165, People's Republic of China
- ⁴⁰ Shandong Normal University, Jinan 250014, People's Republic of China
- ⁴¹ Shandong University, Jinan 250100, People's Republic of China
- ⁴² Shanghai Jiao Tong University, Shanghai 200240, People's Republic of China
- ⁴³ Shanxi Normal University, Linfen 041004, People's Republic of China
- ⁴⁴ Shanxi University, Taiyuan 030006, People's Republic of China
- ⁴⁵ Sichuan University, Chengdu 610064, People's Republic of China
- ⁴⁶ Soochow University, Suzhou 215006, People's Republic of China
- ⁴⁷ South China Normal University, Guangzhou 510006, People's Republic of China
- ⁴⁸ Southeast University, Nanjing 211100, People's Republic of China
- ⁴⁹ State Key Laboratory of Particle Detection and Electronics,
Beijing 100049, Hefei 230026, People's Republic of China
- ⁵⁰ Sun Yat-Sen University, Guangzhou 510275, People's Republic of China
- ⁵¹ Suranaree University of Technology, University Avenue 111, Nakhon Ratchasima 30000, Thailand
- ⁵² Tsinghua University, Beijing 100084, People's Republic of China
- ⁵³ Turkish Accelerator Center Particle Factory Group, (A)Istanbul Bilgi University, HEP Res. Cent.,
34060 Eyup, Istanbul, Turkey; (B)Near East University, Nicosia, North Cyprus, Mersin 10, Turkey
- ⁵⁴ University of Chinese Academy of Sciences, Beijing 100049, People's Republic of China
- ⁵⁵ University of Groningen, NL-9747 AA Groningen, The Netherlands
- ⁵⁶ University of Hawaii, Honolulu, Hawaii 96822, USA
- ⁵⁷ University of Jinan, Jinan 250022, People's Republic of China
- ⁵⁸ University of Manchester, Oxford Road, Manchester, M13 9PL, United Kingdom
- ⁵⁹ University of Minnesota, Minneapolis, Minnesota 55455, USA
- ⁶⁰ University of Muenster, Wilhelm-Klemm-Str. 9, 48149 Muenster, Germany
- ⁶¹ University of Oxford, Keble Rd, Oxford, UK OX13RH
- ⁶² University of Science and Technology Liaoning, Anshan 114051, People's Republic of China
- ⁶³ University of Science and Technology of China, Hefei 230026, People's Republic of China
- ⁶⁴ University of South China, Hengyang 421001, People's Republic of China
- ⁶⁵ University of the Punjab, Lahore-54590, Pakistan
- ⁶⁶ University of Turin and INFN, (A)University of Turin, I-10125, Turin, Italy; (B)University
of Eastern Piedmont, I-15121, Alessandria, Italy; (C)INFN, I-10125, Turin, Italy
- ⁶⁷ Uppsala University, Box 516, SE-75120 Uppsala, Sweden
- ⁶⁸ Wuhan University, Wuhan 430072, People's Republic of China
- ⁶⁹ Xinyang Normal University, Xinyang 464000, People's Republic of China
- ⁷⁰ Zhejiang University, Hangzhou 310027, People's Republic of China
- ⁷¹ Zhengzhou University, Zhengzhou 450001, People's Republic of China
- ^a Also at the Moscow Institute of Physics and Technology, Moscow 141700, Russia
- ^b Also at the Novosibirsk State University, Novosibirsk, 630090, Russia
- ^c Also at the NRC "Kurchatov Institute", PNPI, 188300, Gatchina, Russia
- ^d Currently at Istanbul Arel University, 34295 Istanbul, Turkey
- ^e Also at Goethe University Frankfurt, 60323 Frankfurt am Main, Germany
- ^f Also at Key Laboratory for Particle Physics, Astrophysics and Cosmology, Ministry
of Education; Shanghai Key Laboratory for Particle Physics and Cosmology; Institute
of Nuclear and Particle Physics, Shanghai 200240, People's Republic of China
- ^g Also at Key Laboratory of Nuclear Physics and Ion-beam Application (MOE) and Institute
of Modern Physics, Fudan University, Shanghai 200443, People's Republic of China
- ^h Also at Harvard University, Department of Physics, Cambridge, MA, 02138, USA
- ⁱ Also at State Key Laboratory of Nuclear Physics and Technology,
Peking University, Beijing 100871, People's Republic of China
- ^j Also at School of Physics and Electronics, Hunan University, Changsha 410082, China
- ^k Also at Guangdong Provincial Key Laboratory of Nuclear Science, Institute of

Quantum Matter, South China Normal University, Guangzhou 510006, China

^l Also at Frontiers Science Center for Rare Isotopes, Lanzhou University, Lanzhou 730000, People's Republic of China

^m Also at Lanzhou Center for Theoretical Physics, Lanzhou University, Lanzhou 730000, People's Republic of China

The Born cross sections are measured for the first time for the processes $e^+e^- \rightarrow D_s^{*+}D_{s0}^*(2317)^- + c.c.$ and $e^+e^- \rightarrow D_s^{*+}D_{s1}(2460)^- + c.c.$ at the center-of-mass energy $\sqrt{s} = 4.600$ GeV, 4.612 GeV, 4.626 GeV, 4.640 GeV, 4.660 GeV, 4.68 GeV, and 4.700 GeV, and for $e^+e^- \rightarrow D_s^{*+}D_{s1}(2536)^- + c.c.$ at $\sqrt{s} = 4.660$ GeV, 4.680 GeV, and 4.700 GeV, using data samples collected with the BESIII detector at the BEPCII collider. No structures are observed in cross-section distributions for any of the processes.

I. INTRODUCTION

The D_s^+ meson and its excited states are formed from $c\bar{s}$ quark-antiquark pairs. Throughout the paper, charge-conjugation is implied. Three excited P -wave states above the $D^{(*)}K$ threshold have been observed at the CLEO, BABAR, Belle, and BESIII experiments [1–9]. They are referred to as $D_{s0}^*(2317)^+$, $D_{s1}(2460)^+$, and $D_{s1}(2536)^+$, and are assigned the spin-parity quantum numbers J^P as 0^+ , 1^+ , and 1^+ , respectively [10], matching the predictions from the heavy-quark effective theory [11, 12]. Their masses are measured to be (2317.8 ± 0.5) MeV/ c^2 , (2459.5 ± 0.6) MeV/ c^2 , and (2535.11 ± 0.06) MeV/ c^2 , respectively [10]. For the cases of the $D_{s0}^*(2317)^+$ and $D_{s1}(2460)^+$ states, these values are significantly lower than the theoretical predictions for the charmed-strange mesons in the P -wave doublet [13]. The low-mass puzzle of the $D_{s0}^*(2317)^+$ and $D_{s1}(2460)^+$ mesons has inspired various exotic explanations, including tetraquark states [14–19], $D^{(*)}K$ molecule states [20–24], or mixtures of $c\bar{s}$ and $D^{(*)}K$ states [25]. Further experimental measurements are needed in order to elucidate their structures.

Moreover, several charmonium-like Y states with $J^{PC} = 1^{--}$ lying above the open-charm threshold have been discovered, such as the $Y(4260)$ [26–28], $Y(4360)$ [29, 30], and $Y(4660)$ [30]. Since Y states could decay to open-charm meson pairs, exclusive cross section measurements of open-charm meson pair production in e^+e^- collisions will provide further insight on the internal structures of these charmonium-like resonances. Measurements of $e^+e^- \rightarrow D_s^{(*)+}D_s^{(*)-}$ cross sections were performed at Belle [31], BABAR [32], and CLEO [33]. BESIII extended these studies to higher excited states by measuring the cross sections of $e^+e^- \rightarrow D_s^+D_{s1}(2460)^-$ and $e^+e^- \rightarrow D_s^{*+}D_{s1}(2460)^-$ [34] with an integrated luminosity of 859 pb^{-1} at center-of-mass (c.m.) energies \sqrt{s} from 4.467 to 4.600 GeV. In this paper, we report new measurements of the Born cross sections of the processes $e^+e^- \rightarrow D_s^{*+}D_{s0}^*(2317)^-$, $e^+e^- \rightarrow D_s^{*+}D_{s1}(2460)^-$, and $e^+e^- \rightarrow D_s^{*+}D_{s1}(2536)^-$ at BESIII at $\sqrt{s} \geq 4.6$ GeV, and search for possible vector charmonium-like states.

II. DETECTOR, DATA SAMPLES AND MONTE CARLO SIMULATIONS

The BESIII detector located at the Beijing Electron Positron Collider (BEPCII) [35] is a major upgrade of the BESII experiment at the BEPC accelerator [36]. The cylindrical core of the BESIII detector consists of a helium-based multilayer drift chamber (MDC), a plastic scintillator time-of-flight system (TOF), and a CsI(Tl) electromagnetic calorimeter (EMC), which are all enclosed in a superconducting solenoidal magnet providing a 1.0 T magnetic field. The solenoid is supported by an octagonal flux-return yoke with resistive plate counter muon-identifier modules interleaved with steel. The acceptance of charged particles and photons is 93% over the 4π solid angle. The charged-particle momentum resolution at 1 GeV/ c is 0.5%, and the dE/dx resolution is 6% for the electrons from Bhabha scattering. The EMC measures photon energies with a resolution of 2.5% (5%) at 1 GeV in the barrel (end-cap) region. The time resolution of the TOF barrel part is 68 ps. The time resolution of the end cap part was 110 ps before 2015; at that time the end cap TOF system was upgraded with multi-gap resistive plate chambers, and the time resolution improved to 60 ps.

The results reported in this article for the processes $e^+e^- \rightarrow D_s^{*+}D_{s0}^*(2317)^-$ and $e^+e^- \rightarrow D_s^{*+}D_{s1}(2460)^-$ are determined from seven energy points from 4.600 to 4.700 GeV, where the data at 4.600 GeV were accumulated in 2014, and the remainder in 2020. At energies of 4.660 GeV and above, the data are also used to study $e^+e^- \rightarrow D_s^{*+}D_{s1}(2536)^-$. Table I lists the individual c.m. energies and their integrated luminosities.

The GEANT4-based [37] Monte Carlo (MC) simulation framework BOOST [38], which includes the description of the detector geometry and response, is used to produce large simulated event samples. These samples are exploited to optimize the event selection criteria, to determine the detection efficiency, and to evaluate the initial-state radiation (ISR) correction factor $(1 + \delta)$. Exclusive phase space (PHSP) MC samples of $e^+e^- \rightarrow D_s^{*+}D_{s0}^*(2317)^-$, $e^+e^- \rightarrow D_s^{*+}D_{s1}(2460)^-$, and $e^+e^- \rightarrow D_s^{*+}D_{s1}(2536)^-$ are generated using KKMC [39–41], where the effects of ISR and beam-energy spread are taken into account. Generic MC samples of open-charm processes are used to estimate background contribu-

tions. The known decay modes are modeled with BESEVTGEN [42, 43], using branching fractions taken from PDG [10], while the unknown decays of charmonium states are modeled using LUNDCHARM [44]. Final-state radiation effects are simulated by the PHOTOS [45] package. In the signal MC samples, D_s^{*+} are simulated to decay into γD_s^+ , with the subsequent decay of D_s^+ into $K^+K^-\pi^+$, while the $D_{s0}^*(2317)^-$, $D_{s1}(2460)^-$, and $D_{s1}(2536)^-$ mesons decay inclusively. A P -wave model and a Dalitz plot decay model [46–48] are used to simulate $D_s^{*+} \rightarrow \gamma D_s^+$ and $D_s^+ \rightarrow K^+K^-\pi^+$, respectively.

III. SELECTION CRITERIA

The candidate events of $e^+e^- \rightarrow D_s^{*+}D_{s0}^*(2317)^-$, $e^+e^- \rightarrow D_s^{*+}D_{s1}(2460)^-$, and $e^+e^- \rightarrow D_s^{*+}D_{s1}(2536)^-$ are selected with a partial reconstruction method to obtain higher efficiencies. The $D_{s0}^*(2317)^-$, $D_{s1}(2460)^-$, and $D_{s1}(2536)^-$ signals are searched for in the recoil-mass spectrum of D_s^{*+} candidates. The D_s^{*+} candidates are reconstructed via $D_s^{*+} \rightarrow \gamma D_s^+$, while the D_s^+ candidates are reconstructed via $D_s^+ \rightarrow \phi\pi^+$, $\phi \rightarrow K^+K^-$ and $D_s^+ \rightarrow \bar{K}^{*0}K^+$, $\bar{K}^{*0} \rightarrow K^-\pi^+$. Thus, there are three charged tracks from D_s^+ decays and one additional photon candidate from $D_s^{*+} \rightarrow \gamma D_s^+$.

Each track must originate from the interaction point (IP), which means that the distance of the closest approach to the IP of each track is required to be within 10 cm in the beam direction and within 1 cm in the plane perpendicular to the beam direction. Additionally, each track must reside within the active region of the MDC, meaning that its polar angle θ must satisfy $|\cos\theta| < 0.93$. The dE/dx and TOF information are used to perform particle identification (PID). Pion candidates are required to satisfy $\text{Prob}(\pi) > \text{Prob}(K)$ and $\text{Prob}(\pi) > 0.001$, where $\text{Prob}(\pi)$ and $\text{Prob}(K)$ are the PID probabilities for a track to be a pion and kaon, respectively. Kaon candidates are required to satisfy $\text{Prob}(K) > \text{Prob}(\pi)$ and $\text{Prob}(K) > 0.001$. With these PID requirements, the probability of misidentifying a K^+ as π^+ or a π^+ as K^+ is below 3%.

The photon candidates are selected from EMC showers that are not associated with charged tracks. The deposited energy is required to be larger than 25 MeV in the barrel EMC ($|\cos\theta| < 0.8$), or larger than 50 MeV in the end-cap EMC ($0.86 < |\cos\theta| < 0.92$). To eliminate the showers from charged particles, the angle between the photon and the extrapolated impact point of any good charged track at the EMC front face must be larger than 20° . The timing of the shower is required to be within [50, 700] ns after the reconstructed event start time to suppress noise and energy deposits unrelated to the event.

To reconstruct D_s^{*+} mesons, two kaons, one pion, and

one photon candidates are required. All the $K^+K^-\pi^+$ in all combinations of $\gamma K^+K^-\pi^+$, which pass a vertex fit are kept. Mass-constrained fits to the nominal masses of D_s^+ and D_s^{*+} (2C) are performed, and the χ^2 of this fit is required to be less than 10 to suppress the backgrounds. To select $D_s^+ \rightarrow \phi\pi^+$, $\phi \rightarrow K^+K^-$ and $D_s^+ \rightarrow \bar{K}^{*0}K^+$, $\bar{K}^{*0} \rightarrow K^-\pi^+$ submodes, the invariant masses of K^+K^- and $K^-\pi^+$ are required to satisfy $|M(K^+K^-) - m_\phi| < 9 \text{ MeV}/c^2$ and $|M(K^-\pi^+) - m_{\bar{K}^{*0}}| < 84 \text{ MeV}/c^2$, respectively, where m_ϕ ($m_{\bar{K}^{*0}}$) is the nominal mass of the ϕ (\bar{K}^{*0}) meson taken from the PDG [10].

IV. MEASUREMENTS OF THE $e^+e^- \rightarrow D_s^{*+}D_{sJ}^-$

The recoil-mass distributions of D_s^{*+} candidates from data samples at $\sqrt{s} = 4.600 \text{ GeV}$, 4.612 GeV , 4.626 GeV , 4.640 GeV , 4.660 GeV , 4.680 GeV , and 4.700 GeV are shown in Fig. 1. To improve the recoil mass resolution, the recoil mass of D_s^{*+} is defined to be $M_{D_s^{*+}}^{\text{rec}} = M_{\gamma K^+K^-\pi^+}^{\text{recoil}} + M(\gamma K^+K^-\pi^+) - m_{D_s^{*+}}$, where $M_{\gamma K^+K^-\pi^+}^{\text{recoil}} = \sqrt{(P_{\text{c.m.}} - P_\gamma - P_{K^+} - P_{K^-} - P_{\pi^+})^2}$. Here $P_{\text{c.m.}}$, P_γ , P_{K^+} , P_{K^-} , and P_{π^+} are the four-momenta of the initial e^+e^- system, the selected γ , K^+ , K^- , and π^+ , respectively, $M(\gamma K^+K^-\pi^+)$ is the invariant mass of the $\gamma K^+K^-\pi^+$ system, and $m_{D_s^{*+}}$ is the nominal mass of the D_s^{*+} meson [10]. Clear signals are seen for the $D_{s1}(2460)^-$ at all of the energy points apart from 4.612 GeV, and are found for the $D_{s1}(2536)^-$ at $\sqrt{s} = 4.660 \text{ GeV}$, 4.680 GeV , and 4.700 GeV , and for the $D_{s0}^*(2317)^-$ at $\sqrt{s} = 4.626 \text{ GeV}$ and 4.680 GeV . Detailed studies of the generic MC samples with a generic event type analysis tool, TopoAna [49], indicate that there are no peaking backgrounds in the signal region. We considered possible contributions of processes such as $e^+e^- \rightarrow D_s^+\gamma D_{sJ}^-$ and $e^+e^- \rightarrow D^0(\rightarrow K^-\pi^+)K^+\gamma D_{s0}^*(2317)^-$ by plotting the recoil mass distributions for events in the D_s^{*+} mass sidebands; no peaking structures were observed. An unbinned maximum-likelihood fit is performed to the D_s^{*+} recoil-mass distributions to determine the signal yields of D_{sJ}^- mesons. The signal probability density function is modeled according to a MC-derived signal shape, while the background is modeled with an ARGUS function [50]. The fitted results are summarized in Fig. 1 and Table I. The $D_{s0}^*(2317)^-$ signal significance of the combined data samples from all energy points is 6.9σ . The signal significances are determined by comparing the log-likelihood values with and without including a D_{sJ}^- signal in the fit, taking the change in the number of degrees-of-freedom into account.

Since the statistical significances of D_{sJ}^- signals at some energy points are less than 3σ , with a uniform prior probability density function, the Bayesian upper limits on the numbers of D_{sJ}^- signal events ($N_{\text{U.L.}}$) are determined at the 90% confidence level (C.L.) by solving the following

equation

$$\int_0^{N_{\text{U.L.}}} \mathcal{L}(x) dx = 0.9 \int_0^{+\infty} \mathcal{L}(x) dx,$$

where x is the assumed yield of the D_{sJ}^- signal and $\mathcal{L}(x)$ is the maximized likelihood of the data assuming x signal events. The results of $N_{\text{U.L.}}$ obtained by using above method are listed in Table I.

The Born cross sections of $e^+e^- \rightarrow D_s^{*+}D_{sJ}^-$ are calculated using the formula

$$\sigma_B(e^+e^- \rightarrow D_s^{*+}D_{sJ}^-) = \frac{N_{\text{fit}}}{\mathcal{L}_{\text{int}}(1+\delta)(1+\delta^{\text{VP}})\epsilon_{D_s^{*+}}}, \quad (1)$$

where N_{fit} is the fitted D_{sJ}^- signal yield, $1+\delta$ is the radiative correction factor obtained from a QED calculation with 1% accuracy [51] using the KKMC generator, $1+\delta^{\text{VP}}$ is the vacuum polarization factor, which is taken from Ref. [52] (δ^{VP} is around 0.055 for all studied energy points), and \mathcal{L}_{int} is the integrated luminosity at each energy point. The D_s^{*+} reconstruction efficiency $\epsilon_{D_s^{*+}}$ is the product of the detection efficiency ϵ and the branching fractions for $D_s^{*+} \rightarrow \gamma D_s^+$ and $D_s^{*+} \rightarrow K^+K^-\pi^+$ (93.5% and 5.39%, respectively [10]). The calculation of the upper limits on Born cross sections at 90% C.L. is performed analogously, replacing N_{fit} with $N_{\text{U.L.}}$.

The measured Born cross sections of $e^+e^- \rightarrow D_s^{*+}D_{sJ}^-$ and the upper limits at 90% C.L. (with systematic uncertainties included) are summarized in Table I. The systematic uncertainties and the method to take them into account in the upper limits are discussed in Sec. V. The Born cross sections, with statistical uncertainties only, are shown in Fig. 2.

V. SYSTEMATIC UNCERTAINTIES

The systematic uncertainties of the measured cross sections of $e^+e^- \rightarrow D_s^{*+}D_{s0}^*(2317)^-$, $e^+e^- \rightarrow D_s^{*+}D_{s1}(2460)^-$, and $e^+e^- \rightarrow D_s^{*+}D_{s1}(2536)^-$ are divided into two categories: multiplicative systematic uncertainties and additive systematic uncertainties. The multiplicative systematic uncertainties are associated with tracking and PID efficiencies, photon-detection efficiency, MC sample size, ISR and vacuum-polarization corrections, measurement of luminosity, the branching fractions of intermediate states, and the kinematic fit. The additive systematic uncertainties are associated with the D_{sJ}^- mass, the background shape, and the fit range.

The uncertainties related to PID and tracking are determined to be 3.0% respectively [53]. The uncertainty of the photon reconstruction efficiency is 1.0%, which is derived from the study of $J/\psi \rightarrow \rho^0(\rightarrow \pi^+\pi^-)\pi^0(\rightarrow \gamma\gamma)$ [54] events. The uncertainties due to finite sizes of the MC samples are determined to be at most 0.9% at

each energy point, which arises from the statistical uncertainty of the selection efficiency measured from these samples. From an MC study, we find that the systematic uncertainty due to the choice of $D_s^+ \rightarrow K^+K^-\pi^+$ decay model is negligible. The shapes of the cross section of the processes $e^+e^- \rightarrow D_s^{*+}D_{sJ}^-$ affect the radiative correction factor and the detection efficiency. Due to the limited number of events in the data sample, a detailed determination of the energy dependence (“line shape”), which would allow for an iterative determination of radiative correction factors, is not possible. Therefore, the input line shapes are changed to a first order polynomial multiplied by $\sqrt{E_m - E_0}$, a function that reasonably describes the shape of available data, where E_m stands for the c.m. energy and E_0 stands for the threshold energy for each process, and the differences in the selection efficiency $\epsilon(1+\delta)$ are taken as the systematic uncertainties. The uncertainty from vacuum polarization is less than 0.1% [52], which is negligible compared to other sources of uncertainties. The integrated luminosities of the data samples are measured using large-angle Bhabha scattering events with an uncertainty less than 1.0%. The uncertainties in the branching fractions $\mathcal{B}(D_s^+ \rightarrow K^+K^-\pi^+)$ and $\mathcal{B}(D_s^{*+} \rightarrow \gamma D_s^+)$ are 2.8% and 0.7% [10], respectively. The uncertainty of the 2C kinematic fit is estimated using control samples of $e^+e^- \rightarrow D_s^{*+}D_s^{*-}$ events at $\sqrt{s} = 4.42$ GeV and 4.6 GeV. The difference between the data and MC efficiencies due to the 2C kinematic fit is 1.7%, which is taken as the systematic uncertainty. Using a control sample of $e^+e^- \rightarrow D_s^{*+}D_s^{*-}$, the mass resolutions of D_s^{*-} candidates between signal MC simulation and data are consistent. Thus, the systematic uncertainty due to mass resolution is negligible.

The uncertainties due to D_{sJ}^- mass are estimated by varying its value by the measured uncertainty [10]. The differences in the fitted D_{sJ}^- signal yields are taken as the systematic uncertainties. Using a control sample of $e^+e^- \rightarrow D_s^{*+}D_s^{*-}$ decays, we find the resolution in missing mass to be essentially the same in data as in the MC, at the current level of statistics. The systematic uncertainties due to fitting itself, the background shape, and the fit range are estimated with a toy MC method. We simulate an ensemble of experiments, generating D_s^{*+} recoil mass distributions based on the nominal fitted results. We generate 1000 distributions and subsequently fit them to obtain D_{sJ}^- signal yields. We plot these results in Gaussian distributions. The difference between the mean values of these distributions and the input signal yields represents the systematic bias or uncertainty due to the fitting procedure. The uncertainty is found to be negligible for all D_{sJ}^- signals. A similar method is used to estimate the systematic uncertainties due to the fit range and the background shape. For the fit range, the lower bound is changed from 2.20 GeV/ c^2 to 2.18 GeV/ c^2 and to 2.22 GeV/ c^2 . For the background shape, instead of an ARGUS function [50], a polynomial $f(M) = (M - M_a)^c(M_b - M)^d$ is used, where M_a and M_b are the lower and upper thresholds of the D_s^{*+} recoil

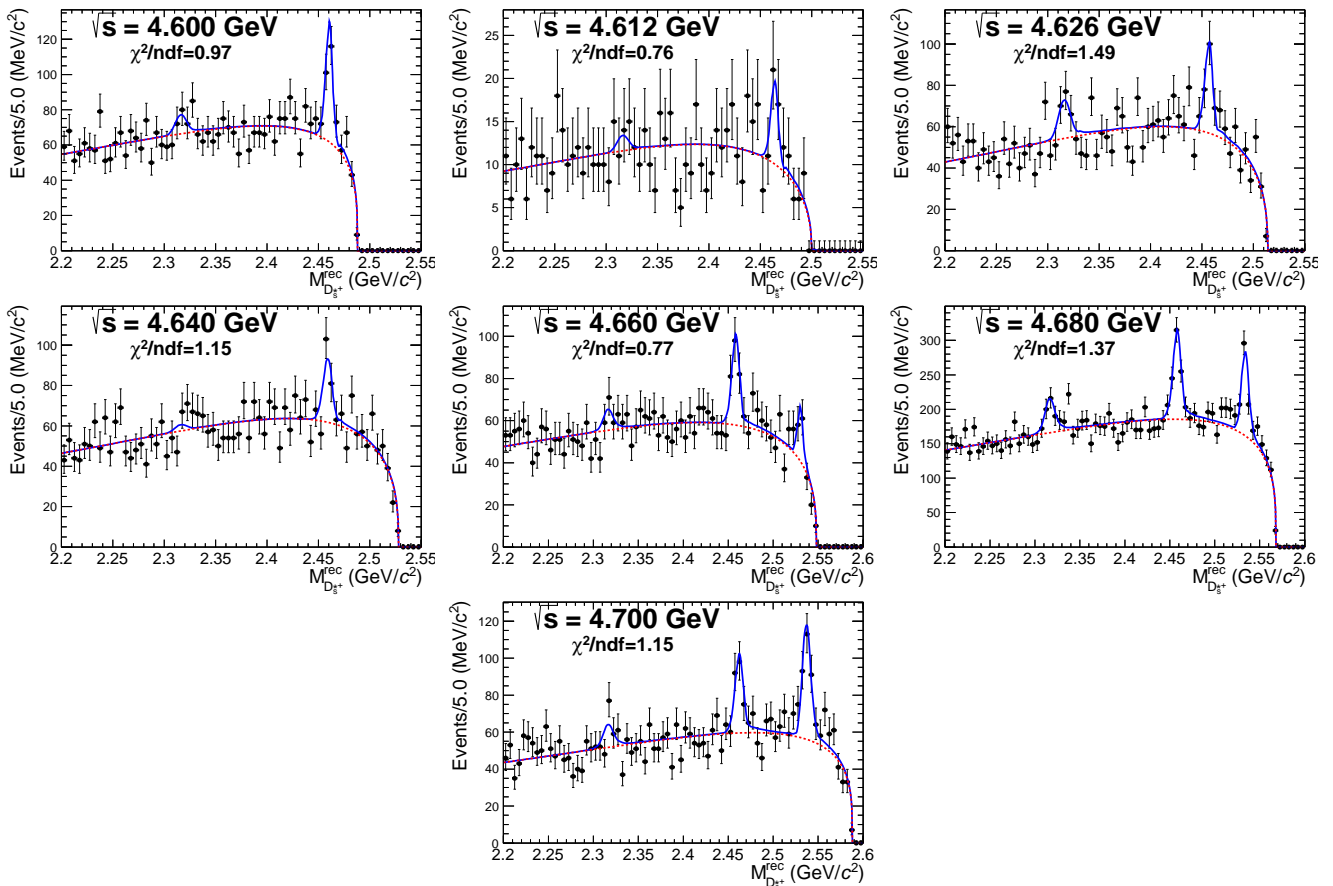


FIG. 1: The recoil-mass distributions of D_s^{*+} candidates from data samples at $\sqrt{s} = 4.600$ GeV, 4.612 GeV, 4.626 GeV, 4.640 GeV, 4.660 GeV, 4.680 GeV, and 4.700 GeV, respectively. The dots with error bars are data and the solid lines are the best fits. Clear $D_{s1}(2460)^-$ signals are observed at all of the energy points except for 4.612 GeV; clear $D_{s1}(2536)^-$ signals are observed at $\sqrt{s} = 4.660$ GeV, 4.680 GeV, and 4.700 GeV; and clear $D_{s0}(2317)^-$ signals are observed at $\sqrt{s} = 4.626$ GeV and 4.680 GeV. The fitted results together with the signal significances are summarized in Table I. The fit quality of $\chi^2/n.d.f.$ is presented in each plot, where *n.d.f.* stands for the number of degrees of freedom.

mass distribution.

For those energy points with a D_{sJ}^- statistical significance larger than 3σ , the central values of the cross section with statistical and systematic uncertainties are reported, and the systematic uncertainties are summarized in Table II. For the other energy points, the upper limits on the cross section at 90% C.L. are reported and the systematic uncertainties are taken into account in two steps. Firstly, among the additive systematic uncertainties described above, the most conservative upper limit at 90% C.L. is kept. Then, to take into account the multiplicative systematic uncertainty, the likelihood curve is convolved with a Gaussian function with a width parameter equal to the corresponding total multiplicative systematic uncertainty. All of the multiplicative systematic uncertainties for the energy points with a D_{sJ}^- signal significance less than 3σ are summarized in Table III. Assuming that all the sources are independent, the total systematic uncertainty is obtained by adding them

in quadrature. The final results of the Born cross section with systematic uncertainties considered are listed in Table I, and shown in Fig. 2 with statistical error bars only.

VI. SUMMARY

In summary, signals are observed in the $e^+e^- \rightarrow D_s^{*+}D_{s0}^-(2317)^-$ process from e^+e^- collision data samples at c.m. energies of 4.626 GeV and 4.68 GeV, in the $e^+e^- \rightarrow D_s^{*+}D_{s1}^-(2460)^-$ process from data samples at c.m. energies of 4.6 GeV, 4.626 GeV, 4.64 GeV, 4.66 GeV, 4.68 GeV, and 4.7 GeV, and the $e^+e^- \rightarrow D_s^{*+}D_{s1}^-(2536)^-$ process from data samples at c.m. energies of 4.66 GeV, 4.68 GeV, and 4.7 GeV, all with statistical significances larger than 3σ . The Born cross sections of these processes are measured for the first time. The results are listed in Table I, and shown in Fig. 2 with statistical er-

TABLE I: Summary of the measured Born cross sections for $e^+e^- \rightarrow D_s^{*+}D_{s0}^*(2317)^-$, $e^+e^- \rightarrow D_s^{*+}D_{s1}(2460)^-$, and $e^+e^- \rightarrow D_s^{*+}D_{s1}(2536)^-$. Listed in the table are the integrated luminosity \mathcal{L}_{int} , the signal efficiency ϵ from signal MC sample, the number of fitted D_{sJ}^- signal events N_{fit} , the upper limit at 90% C.L. on the number of fitted D_{sJ}^- signal yields $N_{\text{U.L.}}$, the ISR radiative correction factor $(1 + \delta)$, the statistical signal significance, and the measured Born cross section (σ_B) and its upper limit ($\sigma_B^{\text{U.L.}}$) at 90% C.L..

\sqrt{s} (GeV)	\mathcal{L}_{int} (pb $^{-1}$)	ϵ (%)	N_{fit}	$N_{\text{U.L.}}$	$(1 + \delta)$	significance	σ_B ($\sigma_B^{\text{U.L.}}$) (pb)
$e^+e^- \rightarrow D_s^{*+}D_{s0}^*(2317)^- + c.c.$							
4.600	586.89	14.1	$25.7^{+19.1}_{-18.3}$	52.0	0.821	1.4σ	$6.8^{+5.0}_{-4.8}$ (14.8)
4.612	102.50	13.7	$9.5^{+8.6}_{-7.8}$	22.0	0.826	1.2σ	$14.7^{+13.3}_{-12.0}$ (34.7)
4.626	511.06	13.7	62.9 ± 18.8	...	0.830	3.6σ	$19.3 \pm 5.8 \pm 2.0$
4.640	541.37	13.8	$20.8^{+18.1}_{-17.3}$	46.4	0.834	1.2σ	$6.0^{+5.2}_{-5.0}$ (14.1)
4.660	523.63	13.9	$20.0^{+18.2}_{-17.2}$	45.6	0.838	1.2σ	$5.8^{+5.3}_{-5.0}$ (14.1)
4.680	1643.38	14.0	151.9 ± 33.2	...	0.845	4.9σ	$13.9 \pm 3.0 \pm 1.4$
4.700	526.20	13.8	$47.5^{+19.5}_{-18.6}$	73.6	0.849	2.7σ	$13.7^{+5.6}_{-5.4}$ (21.4)
$e^+e^- \rightarrow D_s^{*+}D_{s1}(2460)^- + c.c.$							
4.600	586.89	14.1	107.6 ± 17.8	...	0.743	7.1σ	$31.2 \pm 5.2 \pm 3.7$
4.612	102.50	13.7	$15.8^{+7.7}_{-7.0}$	26.8	0.766	2.5σ	$26.1^{+12.8}_{-11.5}$ (44.4)
4.626	511.06	13.5	88.2 ± 18.3	...	0.783	5.6σ	$29.1 \pm 6.0 \pm 2.6$
4.640	541.37	13.6	75.2 ± 18.3	...	0.796	4.7σ	$22.8 \pm 5.6 \pm 2.3$
4.660	523.63	13.5	100.6 ± 19.3	...	0.811	6.1σ	$31.1 \pm 6.0 \pm 2.7$
4.680	1643.38	14.0	339.0 ± 35.0	...	0.822	11.0σ	$31.9 \pm 3.3 \pm 2.5$
4.700	526.20	13.7	103.4 ± 20.2	...	0.831	5.8σ	$30.8 \pm 6.0 \pm 2.6$
$e^+e^- \rightarrow D_s^{*+}D_{s1}(2536)^- + c.c.$							
4.660	523.63	13.8	35.0 ± 11.5	...	0.639	3.4σ	$13.4 \pm 4.4 \pm 1.7$
4.680	1643.38	13.9	243.7 ± 27.9	...	0.706	10.1σ	$26.9 \pm 3.1 \pm 2.3$
4.700	526.20	14.0	109.7 ± 18.7	...	0.753	7.0σ	$35.1 \pm 6.0 \pm 3.0$

TABLE II: Summary of the systematic uncertainties (%) in $\sigma_B(e^+e^- \rightarrow D_s^{*+}D_{sJ}^-)$ for those energy points with statistical significances larger than 3σ .

Sources / \sqrt{s} (GeV)	$D_{s0}^*(2317)^-$		$D_{s1}(2460)^-$					$D_{s1}(2536)^-$			
	4.626	4.680	4.600	4.626	4.640	4.660	4.680	4.700	4.660	4.680	4.700
Tracking, PID and photon detection	7.0	7.0	7.0	7.0	7.0	7.0	7.0	7.0	7.0	7.0	7.0
MC statistics	0.9	0.8	0.8	0.9	0.9	0.9	0.8	0.9	0.9	0.8	0.8
Kinematic fit	1.7	1.7	1.7	1.7	1.7	1.7	1.7	1.7	1.7	1.7	1.7
D_{sJ}^- mass	5.1	3.9	1.5	1.7	3.0	2.3	0.7	2.2	4.7	2.1	1.3
Fit range	3.2	2.9	6.2	0.4	2.1	2.6	0.9	1.5	8.1	1.5	1.5
Background shape	2.4	2.4	5.2	3.2	4.5	0.1	0.2	1.5	2.3	1.6	2.4
ISR radiative correction	2.5	2.7	3.2	2.3	1.8	1.0	0.1	0.9	3.6	1.9	0.8
Luminosity	1.0	1.0	1.0	1.0	1.0	1.0	1.0	1.0	1.0	1.0	1.0
Branching fraction	2.8	2.8	2.8	2.8	2.8	2.8	2.8	2.8	2.8	2.8	2.8
Total	10.5	9.9	11.8	9.0	9.9	8.6	7.9	8.5	13.0	8.6	8.5

TABLE III: Summary of the multiplicative systematic uncertainties (%) in $\sigma_B(e^+e^- \rightarrow D_s^{*+}D_{sJ}^-)$ for those energy points with statistical significances less than 3σ .

Sources / \sqrt{s} (GeV)	$D_{s0}^*(2317)^-$					$D_{s1}(2460)^-$
	4.600	4.612	4.640	4.660	4.700	4.612
Tracking, PID and photon detection	7.0	7.0	7.0	7.0	7.0	7.0
MC statistics	0.8	0.9	0.9	0.8	0.9	0.9
Kinematic fit	1.7	1.7	1.7	1.7	1.7	1.7
ISR radiative correction	2.5	7.3	2.8	2.4	2.5	5.0
Luminosity	1.0	1.0	1.0	1.0	1.0	1.0
Branching fraction	2.8	2.8	2.8	2.8	2.8	2.8
Total	8.3	10.7	8.4	8.2	8.3	9.3

ror bars only. No significant structures are observed in the measured cross sections.

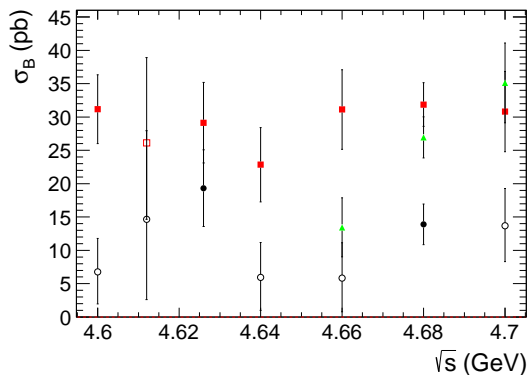


FIG. 2: The Born cross sections of $e^+e^- \rightarrow D_s^{*+}D_{s0}^{*-}(2317)^-$ (the dots with error bars), $e^+e^- \rightarrow D_s^{*+}D_{s1}(2460)^-$ (the rectangles with error bars), and $e^+e^- \rightarrow D_s^{*+}D_{s1}(2536)^-$ (the triangles with error bars) from 4.6 GeV to 4.7 GeV, where the error bars are statistical only. The energy points with signal significances less than 3σ are marked empty, and the upper limits at 90% C.L. on their cross sections are given in Table I.

VII. ACKNOWLEDGEMENT

The BESIII collaboration thanks the staff of BEPCII and the IHEP computing center for their strong sup-

port. This work is supported in part by National Key R&D Program of China under Contracts Nos. 2020YFA0406300, 2020YFA0406400; National Natural Science Foundation of China (NSFC) under Contracts Nos. 11625523, 11635010, 11735014, 11822506, 11835012, 11935015, 11935016, 11935018, 11961141012, 12022510, 12025502, 12035009, 12035013, 12061131003; the Chinese Academy of Sciences (CAS) Large-Scale Scientific Facility Program; Joint Large-Scale Scientific Facility Funds of the NSFC and CAS under Contracts Nos. U1732263, U1832207; CAS Key Research Program of Frontier Sciences under Contract No. QYZDJ-SSW-SLH040; 100 Talents Program of CAS; INPAC and Shanghai Key Laboratory for Particle Physics and Cosmology; ERC under Contract No. 758462; European Union Horizon 2020 research and innovation programme under Contract No. Marie Skłodowska-Curie grant agreement No 894790; German Research Foundation DFG under Contracts Nos. 443159800, Collaborative Research Center CRC 1044, FOR 2359, FOR 2359, GRK 214; Istituto Nazionale di Fisica Nucleare, Italy; Ministry of Development of Turkey under Contract No. DPT2006K-120470; National Science and Technology fund; Olle Engkvist Foundation under Contract No. 200-0605; STFC (United Kingdom); The Knut and Alice Wallenberg Foundation (Sweden) under Contract No. 2016.0157; The Royal Society, UK under Contracts Nos. DH140054, DH160214; The Swedish Research Council; U. S. Department of Energy under Contracts Nos. DE-FG02-05ER41374, DE-SC-0012069

-
- [1] D. Besson *et al.* (CLEO Collaboration), Phys. Rev. D **68**, 032002 (2003).
- [2] P. Avery *et al.* (CLEO Collaboration), Phys. Rev. D **41**, 774 (1990).
- [3] B. Aubert *et al.* (BABAR Collaboration), Phys. Rev. Lett. **90**, 242001 (2003).
- [4] B. Aubert *et al.* (BABAR Collaboration), Phys. Rev. Lett. **93**, 181801 (2004).
- [5] M. Bondioli *et al.* (BABAR Collaboration), Nucl. Phys. B (Proc. Suppl.) **133**, 158 (2004).
- [6] J. P. Lees *et al.* (BABAR Collaboration), Phys. Rev. D **83**, 072003 (2011).
- [7] P. Krokovny *et al.* (Belle Collaboration), Phys. Rev. Lett. **91**, 262002 (2003).
- [8] P. Krokovny *et al.* (Belle Collaboration), Phys. Rev. Lett. **91**, 262002 (2003).
- [9] M. Ablikim *et al.* (BESIII Collaboration), Chin. Phys. C **43**, 031001 (2019).
- [10] P. A. Zyla *et al.* (Particle Data Group), Prog. Theor. Exp. Phys. **2020**, 083C01 (2020)
- [11] Y. B. Dai, C. S. Huang, C. Liu, and S. L. Zhu, Phys. Rev. D **68**, 114011 (2003).
- [12] J. Zeng, J. W. Van Orden, and W. Roberts, Phys. Rev. D **52**, 5229 (1995).
- [13] H. X. Chen, W. Chen, X. Liu, Y. R. Liu, and S. L. Zhu, Rep. Prog. Phys. **80**, 076201 (2017).
- [14] H. Y. Cheng and W. S. Hou, Phys. Lett. B **566**, 193 (2003).
- [15] V. Dmitrasinovic, Phys. Rev. D **70**, 096011 (2004).
- [16] V. Dmitrasinovic, Phys. Rev. D **86**, 016006 (2012).
- [17] V. Dmitrasinovic, Phys. Rev. Lett. **94**, 162002 (2005).
- [18] L. Maiani, F. Piccinini, A. D. Polosa, and V. Riquer, Phys. Rev. D **71**, 014028 (2005).
- [19] Z. G. Wang and S. L. Wan, Nucl. Phys. A **778**, 22 (2006).
- [20] T. Barnes, F. E. Close, and H. J. Lipkin, Phys. Rev. D **68**, 054006 (2003).
- [21] Y. Q. Chen and X. Q. Li, Phys. Rev. Lett. **93**, 232001 (2004).
- [22] Z. X. Xie, G. Q. Feng, and X. H. Guo, Phys. Rev. D **81**, 036014 (2010).
- [23] G. Q. Feng, X. H. Guo, and Z. H. Zhang, Eur. Phys. J. C **72**, 2033 (2012).
- [24] P. Wang and X. G. Wang, Phys. Rev. D **86**, 014030 (2012).
- [25] T. E. Browder, S. Pakvasa, and A. A. Petrov, Phys. Lett. B **578**, 365 (2004).
- [26] B. Aubert *et al.* (BABAR Collaboration), Phys. Rev. Lett. **95**, 142001 (2005).

- [27] T. E. Coan *et al.* (CLEO Collaboration), Phys. Rev. Lett. **96**, 162003 (2006).
- [28] C. Z. Yuan *et al.* (Belle Collaboration), Phys. Rev. Lett. **99**, 182004 (2007).
- [29] B. Aubert *et al.* (BABAR Collaboration), Phys. Rev. Lett. **98**, 212001 (2007).
- [30] X. L. Wang, *et al.* (Belle Collaboration), Phys. Rev. Lett. **99**, 142002 (2007).
- [31] G. Pakhlova *et al.* (Belle Collaboration), Phys. Rev. D **83**, 011101 (2011).
- [32] P. del Amo Sanchez *et al.* (BABAR Collaboration), Phys. Rev. D **82**, 052004 (2010).
- [33] D. Cronin-Hennessy *et al.* (CLEO Collaboration), Phys. Rev. D **80**, 072001 (2009).
- [34] M. Ablikim *et al.* (BESIII Collaboration), Phys. Rev. D **101**, 112008 (2020).
- [35] M. Ablikim *et al.* (BESIII Collaboration), Nucl. Instrum. Method Phys. Res. A **614**, 345 (2010).
- [36] J. Z. Bai *et al.* (BESIII Collaboration), Nucl. Instrum. Method Phys. Res. A **344**, 319 (1994).
- [37] S. Agostinelli *et al.* (GEANT4 Collaboration), Nucl. Instrum. Method Phys. Res. Sect. A **506**, 250 (2003).
- [38] Z. Y. Deng *et al.*, Chin. Phys. C **30**, 371 (2006).
- [39] S. Jadach, B. F. L. Ward, and Z. Was, Comput. Phys. Commun. **130**, 260 (2000).
- [40] R. G. Ping, Chin. Phys. C **38**, 083001 (2014).
- [41] S. Jadach, B. F. L. Ward, and Z. Was, Phys. Rev. D **63**, 113009 (2001).
- [42] R. G. Ping, Chin. Phys. C **32**, 599 (2008).
- [43] D. J. Lange, Nucl. Instrum. Methods Phys. Res., Sect. A **462**, 152 (2001).
- [44] J. C. Chen, G. S. Huang, X. R. Qi, D. H. Zhang and Y. S. Zhu, Phys. Rev. D **62**, 034003 (2000); R. L. Yang, R. G. Ping and H. Chen, Chin. Phys. Lett. **31**, 061301 (2014).
- [45] P. Golonka and Z. Was, Eur. Phys. J. C **45**, 97 (2006).
- [46] R. E. Mitchell *et al.* (CLEO Collaboration), Phys. Rev. D **79**, 072008 (2009).
- [47] M. Ablikim *et al.* (BESIII Collaboration), [arXiv:2011.08041v3](https://arxiv.org/abs/2011.08041v3) [hep-ex]
- [48] P. del A. Sanchez *et al.* (BaBar Collaboration), Phys. Rev. D **83**, 052001 (2011).
- [49] X. Y. Zhou, S. X. Du, G. Li, and C. P. Shen, Comput. Phys. Commun. **258**, 107540 (2021).
- [50] H. Albrecht *et al.* (ARGUS Collaboration), Phys. Lett. B **340**, 217 (1994).
- [51] E. A. Kuraev and V. S. Fadin, Yad. Fiz. **41**, 733 (1985).
- [52] F. Jegerlehner, Nuovo Cim. C **034S1**, 31 (2011).
- [53] M. Ablikim *et al.* (BESIII Collaboration), [arXiv:2011.07855v1](https://arxiv.org/abs/2011.07855v1) [hep-ex].
- [54] M. Ablikim *et al.* (BESIII Collaboration), Phys. Rev. D **81**, 052005 (2010).